Naval Information Warfare Center PACIFIC

TECHNICAL REPORT 3262
FEBRUARY 2022

Active Amplitude and Frequency Control for Frequency Modulated Gyroscopes: Components of Enabling High Stability Frequency Modulated Inertial Sensors

Andrew Sabater
Eric Bozeman
NIWC Pacific

Naval Information Warfare Center Pacific (NIWC Pacific)
San Diego, CA 92152-5001

This page is intentionally blank.

TECHNICAL REPORT 3262
FEBRUARY 2022

Active Amplitude and Frequency Control for Frequency Modulated Gyroscopes: Components of Enabling High Stability Frequency Modulated Inertial Sensors

Andrew Sabater
Eric Bozeman
NIWC Pacific

Administrative Notes:
This REPORT was approved through the Release of Scientific and Technical Information (RSTI) process in September 2021 and formally published in the Defense Technical Information Center (DTIC) in February 2022

NIWC Pacific
San Diego, CA 92152-5001

NIWC Pacific
San Diego, California 92152-5001

A. D. Gainer, CAPT, USN
Commanding Officer

W. R. Bonwit
Executive Director

ADMINISTRATIVE INFORMATION

The work described in this report was performed by the Nonlinear Dynamics and Materials Research Branch (71780) of the Basic and Applied Research Division, Naval Information Warfare Center Pacific (NIWC Pacific), San Diego, CA. The NIWC Pacific In-House Laboratory Independent Research (ILIR) Program provided funding for this Basic Research project.

Released by
John deGrassie, Division Head
Basic and Applied Research

Under authority of
Carly Jackson, Department Head
Cyber, Science and Technology

ACKNOWLEDGMENTS

Editor: RJP

EXECUTIVE SUMMARY

Frequency modulated (FM) gyroscopes have been reported to either have excellent short-term and long-term stability depending on the implementation. This trade-off between short-term stability and long-term stability may be related to design choices with sub-systems for amplitude and frequency control. This work is focused on empirically studying the impact of amplitude and frequency control. Prior to results, background information on amplitude and frequency control are presented. The results section is composed to two sections. The first section is on the impact of the inclusion of integral control to maintain a given amplitude. It is found that adding integral control both improves amplitude matching, as quantified by scale factor, and long-term zero rate output stability. The second section is on the addition of frequency control. With a combination of active amplitude and frequency control, non-stationary noise processes are removed from the rate estimate. While the addition of frequency control does not improve the raw zero rate bias instability, during time periods of low temperature variation, the output can be easily compensated for by using the control voltages to maintain constant frequency. Once compensated, the output can be further filtered using autoregressive methods to remove correlated noise processes. As an added benefit, this filtering helps to reduce angle random walk (ARW). This filtered output demonstrates a bias instability of 0.2 deg/hr at 1,000 sec. With future plans to both improve the resolution of the frequency detector and add active temperature control, it is expected that navigation-grade performance should be possible with the current sub-2 mm by 2 mm dies.

This page is intentionally blank.

CONTENTS

Figures

This page is intentionally blank

1. INTRODUCTION

Frequency modulated (FM) gyroscopes have demonstrated both excellent short-term and long-term stability [1], however information related to the needed control circuity is in general opaque. In particular, the two sub-systems of interest are the amplitude control circuit, typically an automatic gain control (AGC) circuit, and if and how frequency is controlled. Some recent works have proposed that as scale factor stability is not improved with amplitude control [2], to reduce power consumption, amplitude control could be removed. Frequency control has been implemented by introducing in-phase forces [3], ignored [4] or not a feature [5], and likely shaped combs [1].

This work aims to empirically study the impact of amplitude and frequency control on the stability of the FM gyroscopes. Prior to the experimental results, background information on frequency and amplitude control are presented. With the goal of not compromising phase noise performance, challenges associated with the design of shaped combs for frequency compensation are discussed. Important factors related to fabrication must be paid attention to so enable proper operation of the shaped combs. Next, the design of the amplitude control circuit is presented. Compared to prior work that explicitly defined the type of amplitude control, this work advocates for proportional-integral-type (PI) control. Before transitioning to experimental results, information on device fabrication and testing are discussed. To support both rapid testing and potential transition, parts were fabricated using a commercialized process. The first section of experimental work is focused on amplitude control. It it found that amplitude control that aims to minimize steady-state error significantly improves long-term stability. This might be an issue unique to nonlinear operation of FM gyroscopes, but frequency control helps to removed non-stationary noise processes from the rate estimate. During time periods of low temperature variation, the error signals from the amplitude and frequency control circuits are corresponding lower. During this period, bias drift can be easily compensated for by using the control voltages used to maintain constant frequencies as during this period bias drift is likely dominated by linear long-term aging effects. By removing this drift and non-stationary noise processes, the remaining noise processes can be removed using autoregressive methods. With the combination of active amplitude and frequency control, bias drift observation and correction using correlated features, and autoregressive modeling, a bias instability of 0.2 deg/hr at 1,000 sec is reported. As frequency resolution is limited by the frequency detector, and consequently the short-term stability, and long-term stability is potentially limited by temperature stability, future work will include increasing the resolution of the frequency detector and adding active temperature control. With these additions, it is expected to enable a sub-2 mm by 2 mm die that was fabricated using commercialized processes to be capable of navigation-grade performance.

This page is intentionally blank

2. FREQUENCY CONTROL

A variety of methods can be used to implement frequency control or tuning of an oscillator or resonator. With single-transistor oscillator typologies, a classic means to pull the frequency is add a series or parallel load capacitor [6]. This approach can work well with quartz oscillators. However, with MEMS oscillators, it is common to implement a differential sensing mechanism to mitigate common-mode noise issues. Adding the needed capacitors to the sensing circuit would be difficult as these capacitors would need to be closely matched. It is also possible that a mismatch of these capacitors could reduce short-term frequency stability. Due to the relationship between phase and frequency, it is important to note that short-term frequency stability is typically quantify by phase noise measurements. As the short-term frequency stability of the oscillator that comprises an FM inertial sensor dictates the sensor's resolution, it is ideal that the frequency compensation method does not degrade stability. With parallel-plate electrostatically transduced MEMS oscillators, it is possible to tune the frequency of the oscillator by adjusting the bias voltage. This method can work well with amplitude modulated gyroscopes where one of the modes (sense mode) is operated with a small amplitude [7]. For FM inertial sensors, it can be challenging to get good phase noise performance with parallel-plate transduction. For a low phase noise design, it is desirable that the amplitude of the oscillator be as large a possible and that the current produced by the resonator be as large as possible. The selection of the capacitive gap for electrostatic detection has competing effects with regards to maximum displacement and current. Moreover, electrostatic transduction provides a means for low-frequency $1/f$ noise (e.g. from the detection electronics) to mix into the carrier sidebands and degrade phase noise [8].

To implement both transduction and frequency control, this work proposes the use of interdigitated combs. As noted in [8], linear transducer capacitance helps to avoid low-frequency noise aliasing. Thus, straight combs are uses for actuation and sensing. For frequency control, "weakening" shaped combs were selected based on practicality of being successfully fabrication using available means [9]. To understand how the force between two interdigitated combs can be used to modify the effective coupling stiffness between the bodies the combs are attached to, see Figure 1 for a representative schematic.

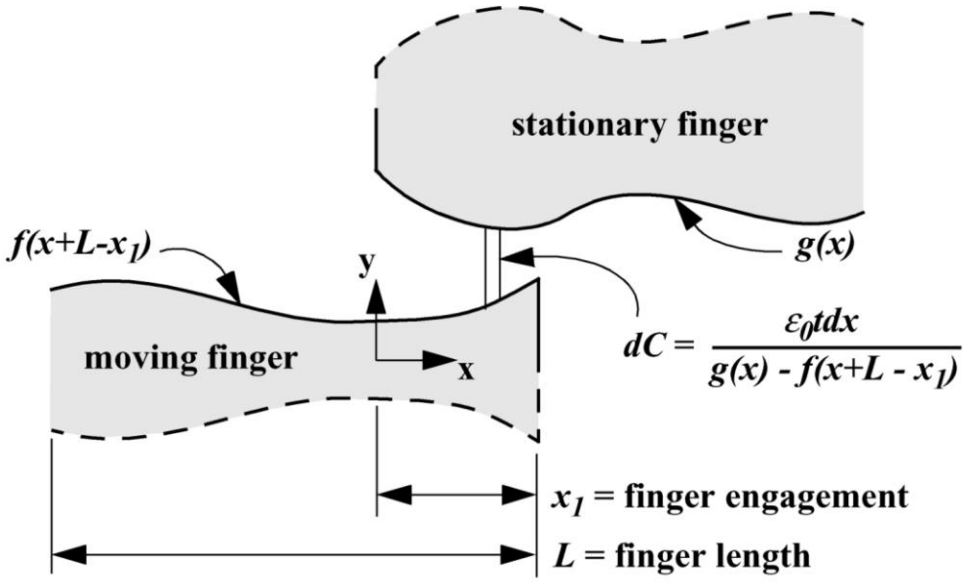

Figure 1. Shaped comb schematic [9].

Neglecting fringe field effects, the force between the two combs in the x direction is

$$F_x = \frac{V^2 \epsilon_0 t}{h(x_1)}, \tag{1}$$

where V is the applied voltage bias, ϵ_0 is the permittivity of free space, t is the out-of-plane thickness of the fingers, and $h(x)$ is the gap profile between fingers. Thus, by the appropriate selection for $h(x)$, one can engineer the fingers to have a specific force profile. As the effective stiffness is proportional to the first spatial derivative of force, one can also select $h(x)$ for a specific stiffness profile. For active frequency control, one can then adjust V to tune the frequency to a desired value. This also requires ones has a means for frequency detection. Frequency counter methods require a high sampling rate in order to have high frequency resolution. This work advocates for the use of phase-locked loop (PLL) methods as the PLL is able to operate at a much lower frequency without compromising frequency resolution. For Lissajous FM gyroscopes [4] or single-resonator, time-switched FM accelerometers [10], inertial sensor information is encoded offset from the oscillator's frequency by some amount (typically 10-100 Hz). In these cases, one may need to low-pass filter the demodulated frequency signal to detect frequency deviation or drift.

Using the notation from [11], the gap profile for softening shaped combs is of the form

$$h(x) = \frac{g_0}{1 + x/x_{ol}}, \tag{2}$$

where g_0 is the gap at the curved finger tip and the straight comb and x_{ol} is the dimensional constant. The selection of these values is dictated by the needed displacement of the oscillator, the utilized fabrication process, and the needed frequency tuning range. For as large as possible for a frequency tuning range, one may seek to minimize both g_0 and x_{ol}. However, as these values decreases, the sensitivity of the design to fabrication issues can become very pronounced. This work proposes that the use of shaped combs for frequency tuning for FM inertial sensors should be for modest frequency tuning to compensate for temperature-induced drift or long-term aging effects.

To consider the design sensitivity to fabrication, it is assumed that the difference between the designed and fabricated part is due to an isotropic over-etch. Shown in Figure 2 is the profile of the shaped comb for the parameters given in [11] as well as an over-etch of 0.2 μm. Figure 3 is the approximate force profile given by $1/h(x)$. The effective stiffness K, estimated from the first derivative from this profile, is shown in the title of figure. While there does appear to be some nonlinearity, it is relatively modest over the designed operating range. The main impact of over-etch for this design is a slight decrease in the effective stiffness. In contrast, shown in Figure 4 is the comb profile from [12]. In that work, a high frequency tuning range was desired due to the relatively high frequency of the sensor. As such, the authors noted the importance of a fabrication process with a sub-micron minimum gap. The issue is that with designing close to the minimum feature size, the design becomes more sensitive to problems such as over-etch. Shown in Figure 5 is the estimated force profile. While this design is approximately 9.63 stiffer, it is about 120.65 times more nonlinear, as assessed by the second-order coefficients of their respective K values. The impact of significant nonlinear effects associated with over-etch is that the tuning range of the combs will be much smaller than expected. In [12], for a 40 V tuning voltage, the designed and measured frequency tuning range was 550 Hz and 80 Hz, respectively. Thus the selection of g_0 and x_{ol} should be made with regards the the frequency compensation goals (i.e. mitigate temperature-induced drift or long-term aging), the needed displacement to reach a given phase noise performance goal, and the limitations of the utilized fabrication process.

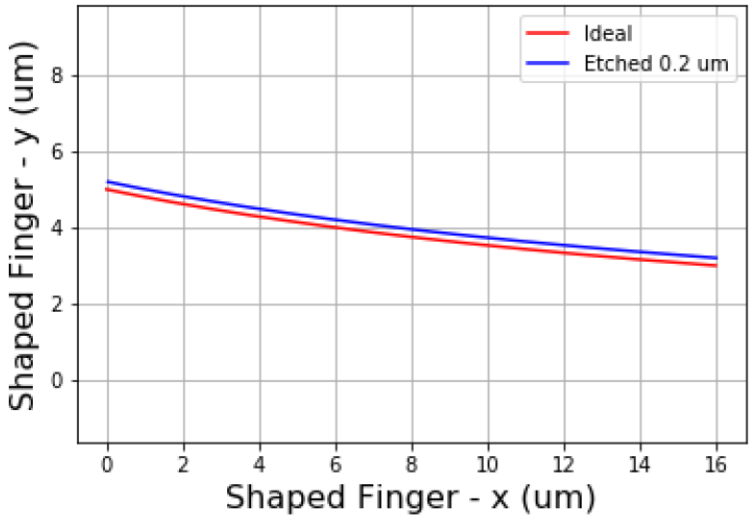

Figure 2. Profile of nominal and over-etched shaped comb from [11].

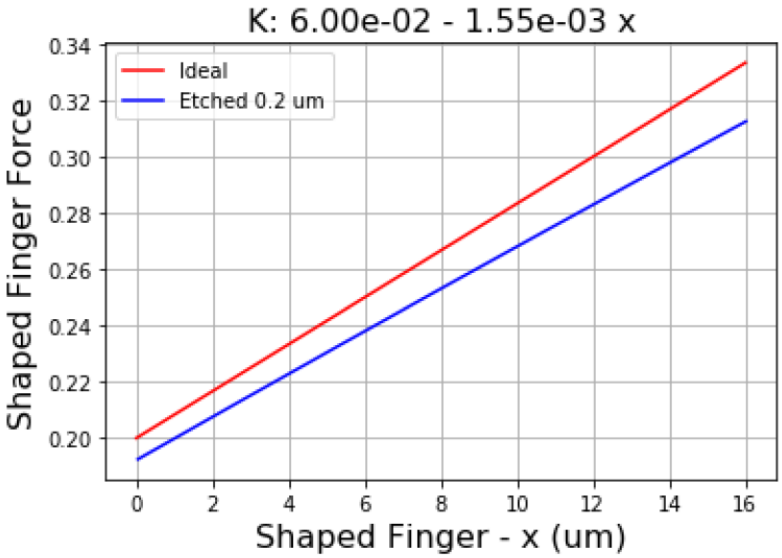

Figure 3. Approximate force profile of nominal and over-etched shaped comb from [11].

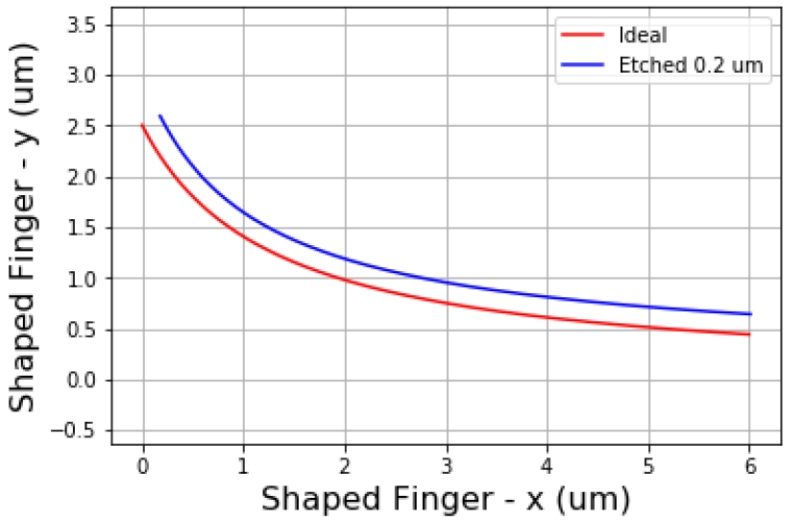

Figure 4. Profile of nominal and over-etched shaped comb from [12].

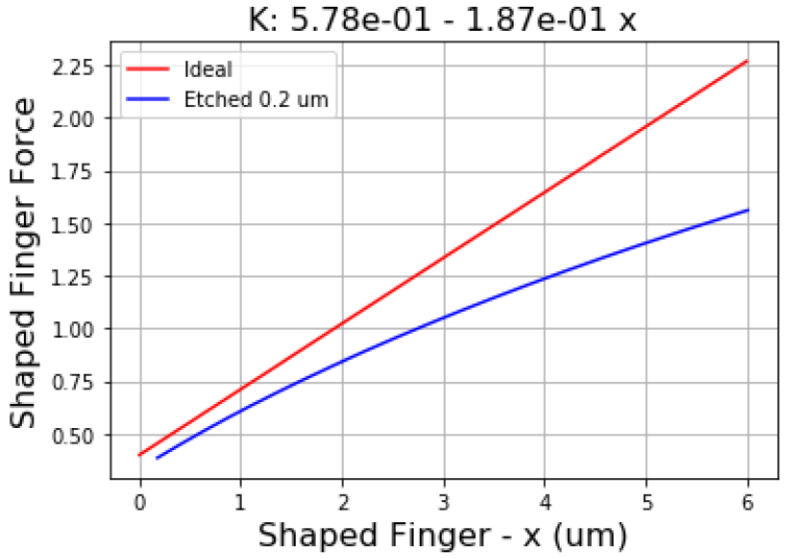

Figure 5. Approximate force profile of nominal and over-etched shaped comb from [12].

3. AMPLITUDE CONTROL

For FM inertial sensors, works have been published that noted both the importance [4] and potential insignificance of amplitude control [2]. In [4], it is claimed that the high scale factor stability of Lissajous FM gyroscopes is due to the relative ease to maintain a constant amplitude. However, [2] empirically found that amplitude control provided no significant improvements to scale factor stability. The exact type of amplitude control implemented in [4] is unknown, but the design of the amplitude gain control (AGC) circuit in [2] is described in [5]. In [5], a proportional-type controller is described that is used the control the amplitude of the oscillator. Based on experiments with a proportional-type controller, the authors of this work advocate for the use of a proportional-integral-type (PI) controller. Results to support this are shown in the following sections. Integral control was added to address steady-state error issues. As will be shown in a later section, simultaneous active amplitude and frequency control implemented to minimize steady-state error (i.e. PI control) provides means to improve stability of FM gyroscopes on all time scales.

A block diagram of the circuit used to maintain oscillations is shown in Figure 6. The fundamental component of the circuit to maintain oscillations is based on the one presented in [13]. It consists of a phase shifter that is connected to comparator. The phase shift produced by the circuit provides a means to optimize phase noise. This phase shift can be implemented various ways, but an active all-pass filter was selected for flexibility. A passive phase shifter or high-pass filter may provide some noise advantages with regards to low-frequency noise from the electronics. The depending on the needed attenuation and the supply voltage limitations of the comparator, an attenuator or the supply voltage can be adjusted to change the amplitude of the output square wave. Automatic amplitude control can be implemented various ways [14], but the approach in this work is relatively similar to [5] by adding a circuit that adjusts the supply limits of the comparator. To measure the amplitude of the input, the rectifier is a “super diode” with a simple RC low-pass filter used to smooth the output [14]. Based on the difference between the measured and desired amplitude, an error signal is generated. This error signal is then used with a PI-type controller that adjusts the supply limits of a comparator.

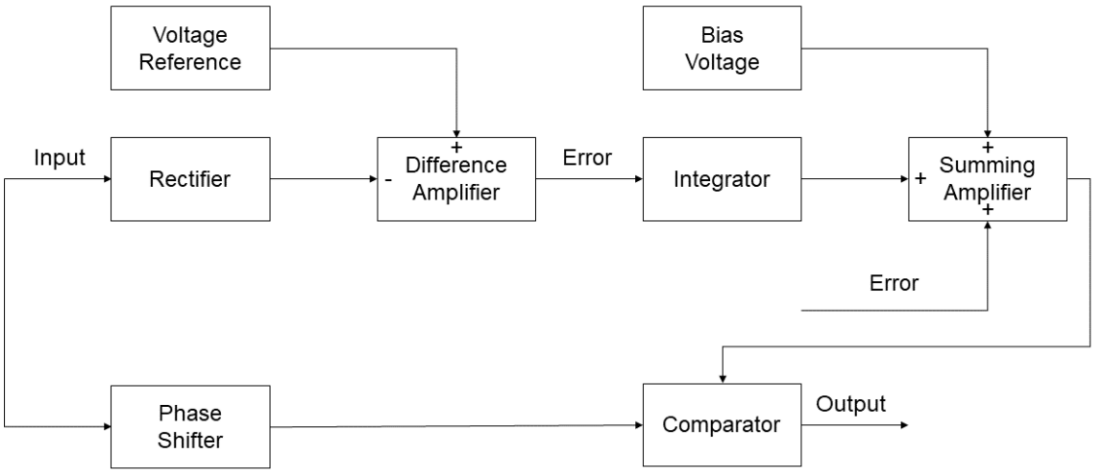

Figure 6. Block diagram of the circuit used to maintain oscillations.

This page is intentionally blank

4. RESONATOR DESIGN AND FABRICATION

To support rapid testing, parts were designed for and fabricated with using MEMSCAP's SOIMUMPS process [15]. In this work, duel pendulum-style resonators similar to [5] or [16] were designed with the addition of shaped combs for frequency compensation. A total die area of 4.5 mm by 4.5 mm was allocated for each part, but the active area was restricted to less than 2 mm by 2 mm to mitigate potential issues during wet release. Based on the design rules of the process of a minimum feature spacing of 3 μm, a mask spot size of 0.25 μm, and potential over-etching of pointed features, the shaped combs were designed considering these limitations. After receiving the parts, they were sent to a local vendor for packaging. The dies were bonded using a cyanoacrylate-based epoxy to a ceramic chip carrier and then wire bonded. For testing, the dies were then placed in the socket of an interface electronics board that was in turn placed in a vacuum chamber. The nominal pressure for most tests was under 10 mTorr. The parts were designed to have matching natural frequencies at about 4.5 kHz. However, due to over-etching, the natural frequency of the parts are closer to 4 kHz with frequency splits ranging from about 20 to 100 Hz. For the device utilized in this work, the frequency split was approximately 68 Hz.

This page is intentionally blank

5. EXPERIMENTAL RESULTS

5.1 P-Type vs. PI-Type AGC

In prior work that explicitly referenced the type of amplitude controller [5], a proportional-type controller was implemented. The assumed amplitude dynamics are of first-order with a time constant equal to Q/ω, where ω is the natural frequency and Q is the quality factor [17]. Thus, in theory, with a very high gain for the proportional controller, the amplitude could settle to the desired value arbitrarily fast and with small steady-state error. However, in practice, due to additional dynamics not captured by a simple first-order process, a high gain can give rise to instability issues. At the cost of increasing the settling time of the controller, adding integral control can address some steady-state error. Tuning the settling time of a PI-type controller to operate close to the settling time of the time constant of the device being controlled can result in both significant overshoot and potential instability. Issues related to overshoot can be observed as modulations in the error of the controller. Provided this modulation frequency is far from the modulation frequency used to detecting rotation, error modulation is typically not an issue, but should be considered.

To quantify amplitude stability, the scale factor of an FM gyroscope is considered of the form

$$SF = \frac{1}{2}\left(\frac{a_1}{a_2} + \frac{a_2}{a_1}\right), \tag{3}$$

where a_1 and a_2 are the amplitudes of the respective oscillators. For Lissajous FM gyroscopes where these amplitudes are intended to be operated with equal amplitude, the scale factor is equal to 1. Shown in Figure 7 is the Allen deviation (ADEV) of the scale factor during trials of using a P-type and PI-type AGC. For the P-type controller, the gain of the controller was set to 50 while the gain of the PI-type controller was set to 10. For the P-type controller, the scale factor exhibits significant drift and the relative amplitude matching (quantified by the value of ADEV) is poor.

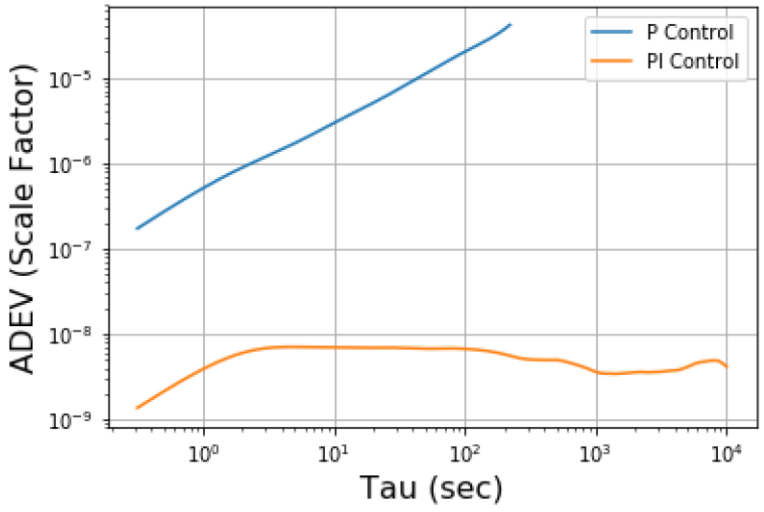

Figure 7. Allen deviation of scale factor during trials of a P-type and PI-type AGC.

Due to operating the gyroscope in a nonlinear regime, there is a coupling between amplitude and frequency. As noted earlier, issues related to overshoot with a PI-controller can result in modulation of the error. This can be observed in the demodulated frequency of the oscillator, which is shown for the cases of a P-type and PI-type controller in Figure 8. The peak at 2 Hz for the PI-type controller is associated with the overshoot of the controller. As 2 Hz is far from 68 Hz, this overshoot does not impact the operation of the sensor.

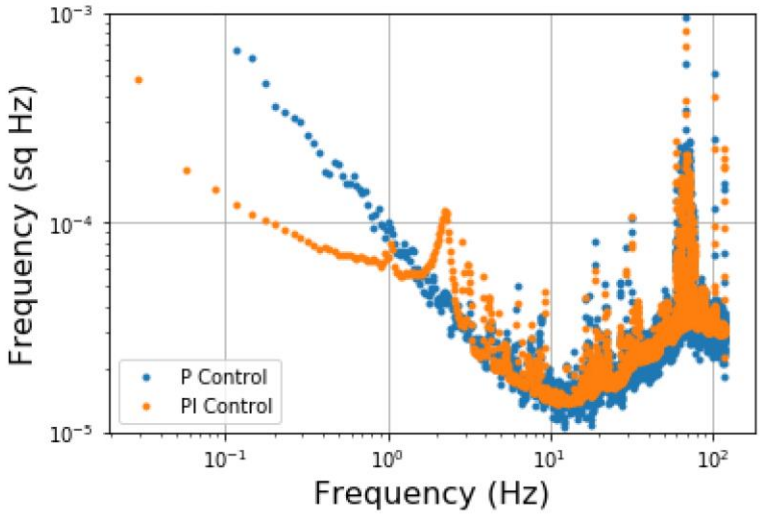

Figure 8. Power spectral density of the demodulated frequency for trials of a P-type and PI-type AGC.

The consequences of improve amplitude stability can be observed in stability in the estimated rate. Shown in Figure 9 is the Allen deviation of the zero rate output for trials with a P-type and PI-type AGC. For the PI-type AGC, the onset of drift occurs at a much longer averaging time.

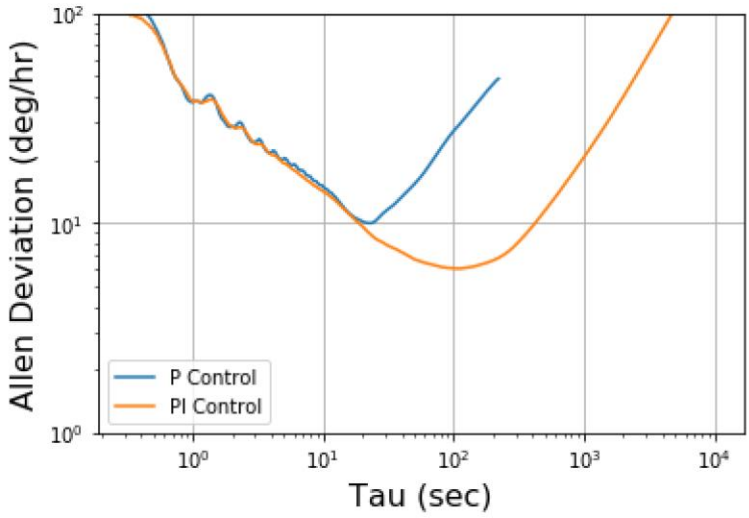

Figure 9. Allen deviation of zero rate output for trials of a P-type and PI-type AGC.

Thus in summary, while adding integral control to maintain a given amplitude increases design complexity and can provide a pathway for noise from the controller to interfere with the operation of the

sensor, integral control greatly improves amplitude stability and significantly improves zero rate output stability.

5.2 ACTIVE FREQUENCY CONTROL

While conducting trials on PI-type AGC control, it was noted that there were correlations between the zero rate output and frequency drift of the constituent oscillators. These relationships are shown in Figure 10. Similar finding had been observed in prior work [18], so one of the motivations of this effort was to determine if active frequency control (in conjunction with active amplitude control) could be used to mitigate zero rate drift. Without the use of other information to track bias drift, active frequency control versus uncontrolled frequency operation does not significantly impact zero rate drift. However, active frequency control helps to remove non-stationary noise processes from the rate estimate. Figure 11 shows the power spectral density of the rate estimate with and without active frequency control. Note the large amount of peaks in the 1 to 10 Hz range for the trial with only a PI-type AGC. While these peaks do not impact the long-term stability of the zero rate output, removal of these peaks are important for application or utilization of the gyroscope as a sensor.

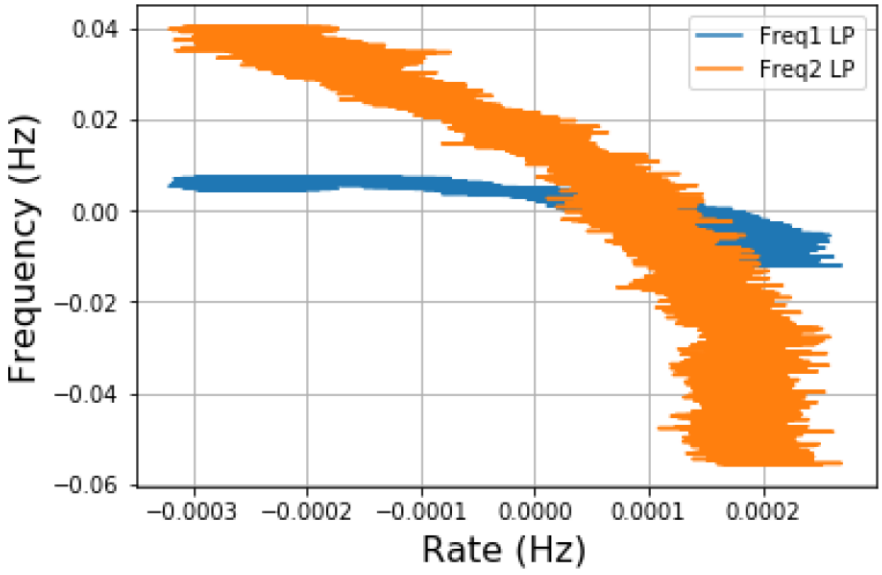

Figure 10. Correlation between zero rate drift and frequency drift.

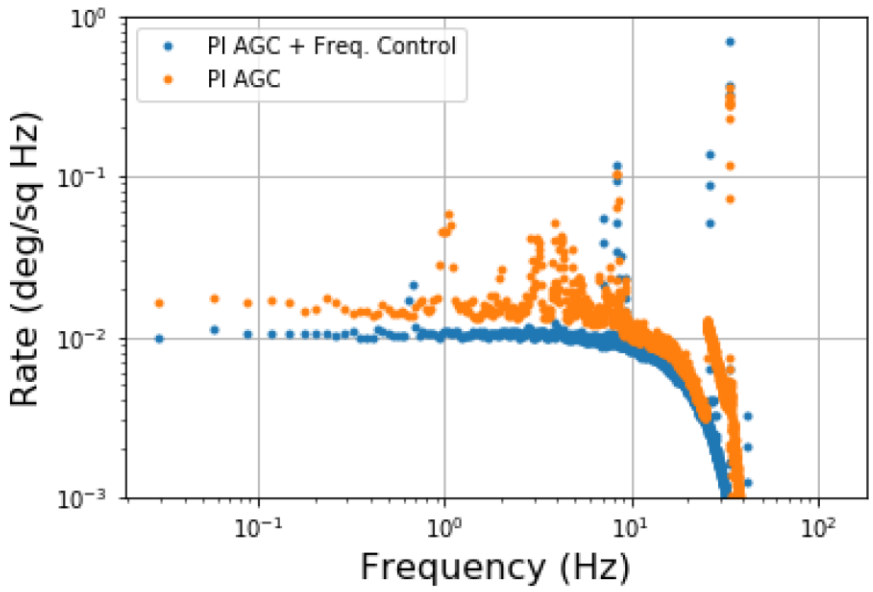

Figure 11. Power spectral density of the rate estimate with and without active frequency control.

During trials conducted over periods of hours, several correlations between rate drift and other features were observed. Prior work noted that drift in quadrature error could be used to correct for bias drift [18]. One limitation with this method is noise from the quadrature error estimate could impact the rate estimate. However, a driving factor that may influence rate drift and it's correlated features could be temperature. Experiments were conducted in a room with air conditioning during certain hours of the day. During the time period when the air conditioning was on and before people entered the room, the amplitude of the oscillators were particularly stable and showed a very small peak to peak variation. Future efforts need to confirm these assumptions, but it is believed that low variations in temperature aid in reducing both amplitude and frequency fluctuations. The amplitude of the oscillators during this time period, with the mean values removed, are shown in Figure 12. For reference, during periods without temperature control, the amplitude may vary about 200 μV. Instead of using quadrature error to observe bias drift, the control voltages used to maintain the oscillators at constant frequencies were used for compensation. Allen deviation of the zero rate outputs, the raw rate estimate with active amplitude and frequency control and one calibrated using the control voltages, are shown in Figure 13. It is important to note that these control voltages are highly correlated with time, but provide a slightly better means for bias compensation as compared to regressing using time. Thus the current hypothesis is that when temperature fluctuations are sufficiently low, drift is dominated by long-term aging effects such as stress relaxation of the epoxy used to bond the dies to the chip carrier.

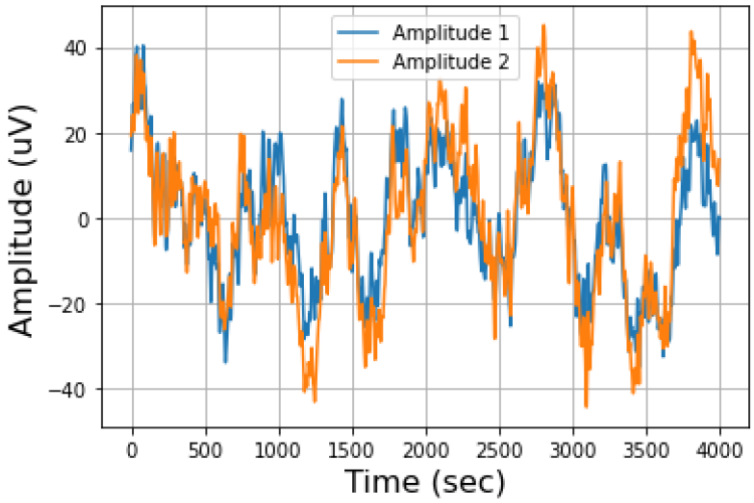

Figure 12. Amplitude of the oscillators (with the mean values removed) with active amplitude and frequency control during a period of low temperature variation.

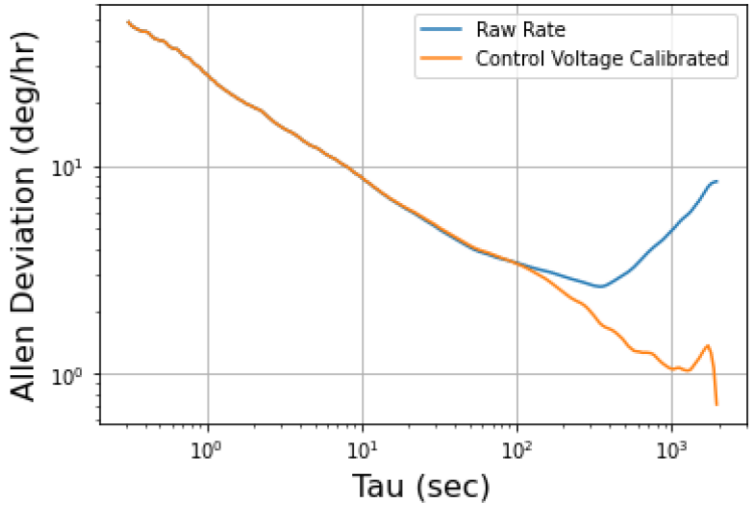

Figure 13. Allen deviation of the raw rate estimate with active amplitude and frequency control and the calibrated output using the control voltages used to maintain constant frequencies.

One significant advantage of active frequency control removing non-stationary noise processes is the output of the sensor can be further filtered using an autoregressive model [19]. Shown in Figure 14 is the time series of the raw output of the device under active amplitude and frequency control, as well as the model residuals from the time periods used for training and tested the model. Balancing the needs of preserving the bandwidth of the sensor and reducing the number of model coefficients, the data was decimated to a lower sampling rate of about 60 Hz. Shown in Figure 15 are the power spectral densities of the raw sensor output and the model residual during the test phase. By using the autoregressive model to remove correlated noise processes, the few remaining peaks in the power spectral density are removed. As an added benefit, the short-term noise, quantified by angle random walk (ARW), is significantly reduced.

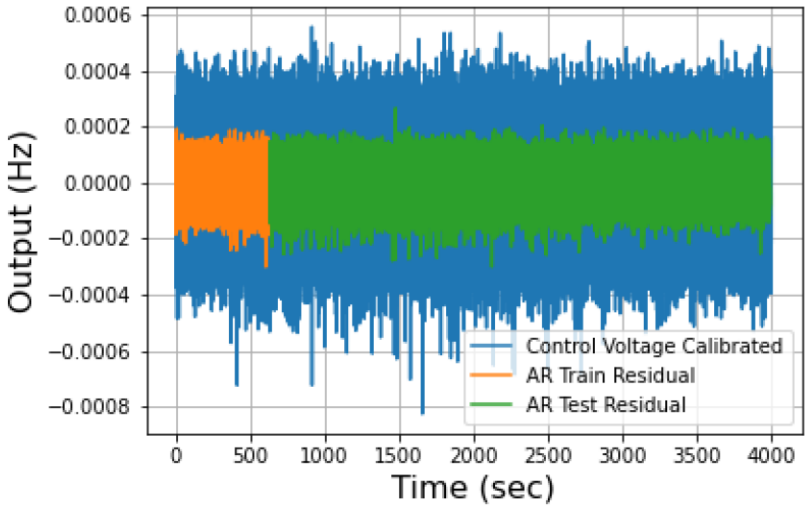

Figure 14. Time series of the raw rate estimate as well as the model residuals from the periods used for training and testing the autoregressive model.

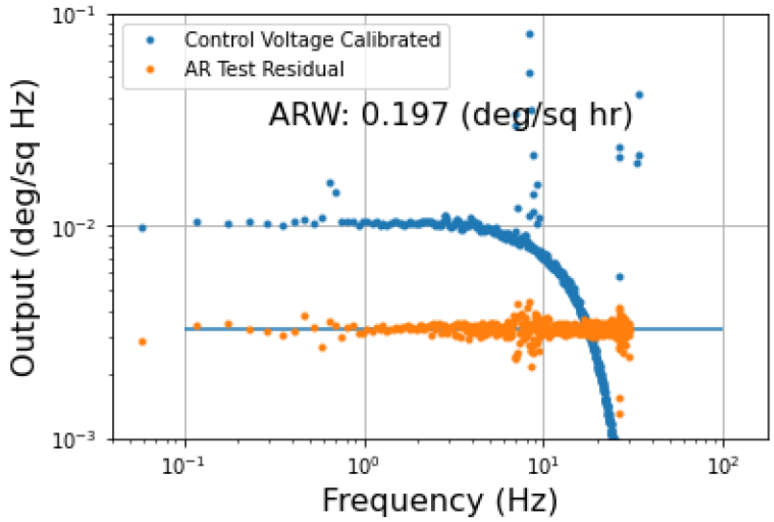

Figure 15. Power spectral density of the raw sensor output and the model residual during the test phase.

Projecting towards future capabilities, shown in Figure 16 is the zero rate output of the calibrated output, the model residual during the test phase, and the white noise fit to model residuals. The bias instability, reported as the minimum value of the Allen deviation, of the model residuals is about 0.2 deg/hr. Provided temperature compensated can be added, the estimated bias instability is projected to be less than 0.1 deg/hr (see ADEV at 10,000 sec). Regardless of which value is used, these results show the pathway to providing stability typically assumed to be very challenging for sub-2 mm by 2 mm dies.

In summary, active frequency control helps to remove non-stationary noise processes from the rate estimate. Without the use of other information correlated with bias drift, active frequency control does not improve bias instability. During time periods of low temperature variation, low amplitude and frequency fluctuations are observed and bias drift exhibits linear drift associated with long-term aging processes.

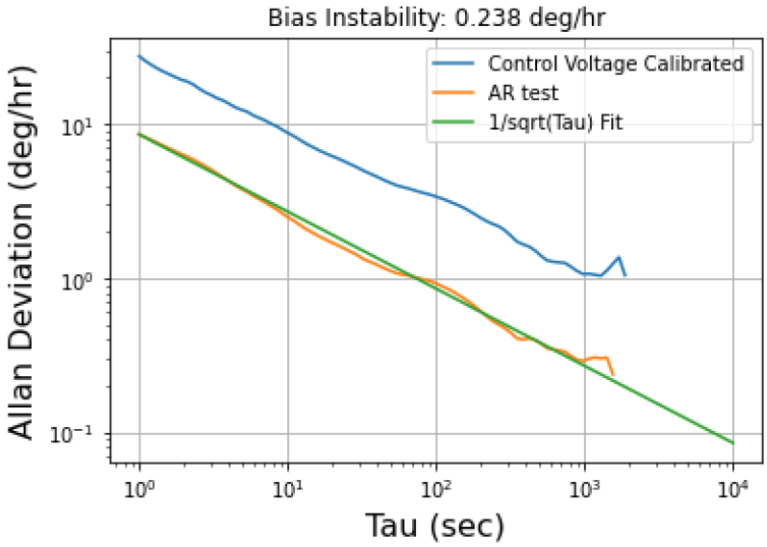

Figure 16. Allen deviation of the calibrated output, the model residuals during the test phase, and the fit to the model residuals.

Under these conditions, for active frequency control, the bias can be easily compensated for with the control voltages used to maintain constant frequencies in a fashion that does not introduce correlated noise. Once calibrated, the remaining correlated noise processes can be filtered out using autoregressive methods. As an added benefit, autoregressive modeling can be used to improve stability on all time scales.

This page is intentionally blank

6. CONCLUSIONS AND FUTURE WORK

With the goal of clarifying impact of amplitude and frequency control on FM gyroscopes, this work empirically studied the impact of different control methods on stability. It is found that amplitude control that significantly improves long-term stability. Adding active frequency control does not improve the uncompensated rate estimate, but it removes uncorrelated noise processes. During time periods of low temperature variation, active amplitude and frequency control stabilizes the rate estimate such that simple methods that utilize processes correlated with bias drift to compensate for this offset. This compensated output can be further filtered using autoregressive methods to remove the remaining correlated noise processes and as a benefit, improve stability on all time scales.

This work focused just on active amplitude and frequency control. To enable navigation-grade performance, future work will focus on improving the resolution of the frequency detector. The frequency detector in this work is limited by the 14-bit ADC (analog to digital converted) on the digital controller [18], however the effective number of bits is closer to 13. This is clear in Figure 8 and is associated with the upward sloping noise floor in the 10 to 100 Hz range. By increasing the resolution of the detector to 24-bits, it is expected that the short-term resolution of the gyroscope will be limited by the phase noise of the oscillator. As referenced in the previous section, low temperature variation enabled methods to improve stability on all time scales. Future plans will include co-packaging dies with components for temperature sensing and heating.

This page is intentionally blank

REFERENCES

1. Eminoglu, B. and Boser, B. E. 2018. "Chopped Rate-to-Digital FM Gyroscope with 40ppm Scale Factor Accuracy and 1.2DPH Bias," *2018 IEEE International Solid - State Circuits Conference - (ISSCC 2018)*, URL https://doi.org/10.1109/ISSCC.2018.8310242.

2. Bordiga, E., Bestetti, M., and Langfelder, G. 2019. "AGC-Less Operation of High-Stability Lissajous Frequency-Modulated Mems Gyroscopes," *2019 20th International Conference on Solid-State Sensors, Actuators and Microsystems & Eurosensors XXXIII (Transducer 2019 - Eurosensors XXXIII)*, URL https://doi.org/10.1109/TRANSDUCERS.2019.8808514.

3. Eminoglu, B., Yeh, Y. C., Izyumin, I. I., Nacita, I., Wireman, M., Reinelt, A., and Boser, B. E. 2016. "Comparison of Long-Term Stability of AM Versus FM Gyroscopes," *2016 IEEE 29th International Conference on Micro Electro Mechanical Systems (MEMS 2016)*, URL https://doi.org/10.1109/MEMSYS.2016.7421790.

4. Izyumin, I. I., Kline, M. H., Yeh, Y.-C., Eminoglu, B., Ahn, C. H., Hong, V. A., Yang, Y., Ng, E. J., Kenny, T. W., and Boser, B. E. 2015. "A 7 PPM, 6 deg/hr Frequency-Output MEMS Gyroscope," *28th IEEE International Conference on Micro Electro Mechanical Systems (MEMS 2015)*, URL https://doi.org/10.1109/MEMSYS.2015.7050879.

5. Minotti, P., Dellea, S., Mussi, G., Bonfanti, A., Facchinetti, S., Tocchio, A., Zega, V., Comi, C., Lacaita, A. L., and Langfelder, G. 2018. "High Scale-Factor Stability Frequency-Modulated MEMS Gyroscope: 3-Axis Sensor and Integrated Electronics Design," *IEEE Transactions on Industrial Electronics*, vol. 65, no. 6, pp. 5040 – 5050.

6. Vittoz, E. 2010. *Low-Power Crystal and MEMS Oscillators: The experience of Watch Developoments*, Springer.

7. Zaman, M. F., Sharma, A., Hao, Z., and Ayazi, F. 2008. "A Mode-Matched Silicon-Yaw Tuning-Fork Gyroscope With Subdegree-Per-Hour Allan Deviation Bias Instability," vol. 17, no. 6, pp. 1526–1536.

8. Kaajakari, V., Koskinen, J. K., and Mattila, T. 2005. "Phase Noise in Capacitively Coupled Micromechanical Oscillators," *IEEE Transaction on Ultrasonics, Ferroelectrics, and Frequency Control*, vol. 52, no. 12, pp. 2322–2331.

9. Jensen, B. D., Mutlu, S., Miller, S., Kurabayashi, K., and Allen, J. J. 2003. "Shaped comb fingers for tailored electromechanical restoring force," *Journal of Microelectromechanical Systems*, vol. 12, no. 3, pp. 373 – 383.

10. Marra, C. R., Ferrari, F. M., Karman, S., Tocchio, A., Rizzini, F., and Langfelder, G. 2018. "Single-resonator, time-switched FM MEMS accelerometer with theoretical offset drift complete cancellation," *31st IEEE International Conference on Micro Electro Mechanical Systems (MEMS 2018)*, URL https://doi.org/10.1109/MEMSYS.2018.8346497.

11. Guo, C. and Fedder, G. K. 2013. "A quadratic-shaped-finger comb parametric resonator," *Journal of Micromechanics and Microengineering*, vol. 23, no. 9, p. 095007.

12. Taheri-Tehrani, P., Defoort, M., Chen, Y., Flader, I., Shin, D. D., Kenny, T. W., and Horsley, D. A. 2017. "Epitaxially-encapsulated quad mass resonator with shaped comb fingers for frequency tuning," *30th IEEE International Conference on Micro Electro Mechanical Systems (MEMS 2017)*, URL https://doi.org/10.1109/MEMSYS.2017.7863608.

13. Sabater, A. B. and Moran, K. M. 2019. "Angle Random Walk Minimization for Frequency Modulated Gyroscopes," *2019 IEEE International Symposium on Inertial Sensors and Systems (IEEE Inertial 2019)*, URL https://doi.org/10.1109/ISISS.2019.8739529.

14. Lee, S. and Nguyen, C. T. C. 2003. "Influence of automatic level control on micromechanical resonator oscillator phase noise," *IEEE International Frequency Control Symposium and PDA Exhibition Jointly with the 17th European Frequency and Time Forum (IEEE EFTF-IFCS 2003)*, URL https://doi.org/10.1109/FREQ.2003.1275113.

15. Cowen, A., Hames, G., Monk, D., Wilcenski, S., and Hardy, B. 2011. *SOIMUMPs Design Handbook*, MEMSCAP Inc., revision 8.0 ed.

16. Kline, M. H., Yeh, Y.-C., Eminoglu, B., Izyumin, I. I., Daneman, M., Horsley, D. A., and Boser, B. E. 2013. "MEMS Gyroscope Bias Drift Cancellation Using Continuous-Time Mode Reversal," *17th International Conference on Solid-State Sensors, Actuators and Microsystems (Transducers & Eurosensors XXVII)*, URL https://doi.org/10.1109/Transducers.2013.6627152.

17. Sabater, A. B., Mora, K. M., Bozeman, E., Wang, A., and Stanzione, K. 2018. "Nonlinear Operation of Inertial Sensors," *Proceedings of the 5th International Conference on Applications in Nonlinear Dynamics (ICAND 2018)*, URL https://link.springer.com/chapter/10.1007/978-3-030-10892-2_11.

18. Sabater, A. B., Bozeman, E., Horta, O., Moran, K. M., and Stanzione, K. 2020. "Quantization Requirements for FM Gyroscopes An Update on the Nonlinear FM Gyroscope," *2020 Joint Conference of the IEEE International Frequency Control Symposium and International Symposium on Applications of Ferroelectrics (IFCS-ISAF 2020)*, URL https://doi.org/10.1109/IFCS-ISAF41089.2020.9234859.

19. Seabold, S. and Perktold, J. 2010. "statsmodels: Econometric and statistical modeling with python," *9th Python in Science Conference*.

INITIAL DISTRIBUTION

71780	A. Sabater	(1)
71780	E. Bozeman	(1)

Defense Technical Information Center
Fort Belvoir, VA 22060–6218 (1)

This page is intentionally blank.

REPORT DOCUMENTATION PAGE

Form Approved
OMB No. 0704-01-0188

PLEASE DO NOT RETURN YOUR FORM TO THE ABOVE ADDRESS.

1. REPORT DATE *(DD-MM-YYYY)*	2. REPORT TYPE	3. DATES COVERED *(From - To)*
FEBRUARY 2022	Final	

4. TITLE AND SUBTITLE

Active Amplitude and Frequency Control for Frequency Modulated Gyroscopes: Components of Enabling High Stability Frequency Modulated Inertial Sensors.

5a. CONTRACT NUMBER

5b. GRANT NUMBER

5c. PROGRAM ELEMENT NUMBER

5d. PROJECT NUMBER

5e. TASK NUMBER

5f. WORK UNIT NUMBER

6. AUTHORS

Andrew Sabater
Eric Bozeman

NIWC Pacific

7. PERFORMING ORGANIZATION NAME(S) AND ADDRESS(ES)

NIWC Pacific
53560 Hull Street
San Diego, CA 92152–5001

8. PERFORMING ORGANIZATION REPORT NUMBER

TR-3262

9. SPONSORING/MONITORING AGENCY NAME(S) AND ADDRESS(ES)

The NIWC Pacific In-House Laboratory Independent Research
53560 Hull Street
San Diego, CA 92152–5001

10. SPONSOR/MONITOR'S ACRONYM(S)

ILIR

11. SPONSOR/MONITOR'S REPORT NUMBER(S)

12. DISTRIBUTION/AVAILABILITY STATEMENT

DISTRIBUTION STATEMENT A: Approved for public release. Distribution is unlimited..

13. SUPPLEMENTARY NOTES

14. ABSTRACT

Frequency modulated (FM) gyroscopes have been reported to either have excellent short-term and long-term stability depending on the implementation. This trade-off between short-term stability and long-term stability may be related to design choices with sub-systems for amplitude and frequency control. This work is focused on empirically studying the impact of amplitude and frequency control. Prior to results, background information on amplitude and frequency control are presented. The results section is composed to two sections. The first section is on the impact of the inclusion of integral control to maintain a given amplitude. It is found that adding integral control both improves amplitude matching, as quantified by scale factor, and long-term zero rate output stability. The second section is on the addition of frequency control. With a combination of active amplitude and frequency control, non-stationary noise processes are removed from the rate estimate. While the addition of frequency control does not improve the raw zero rate bias instability, during time periods of low temperature variation, the output can be easily compensated for by using the control voltages to maintain constant frequency.. Once compensated, the output can be further filtered using autoregressive methods to remove correlated noise processes. As an added benefit, this filtering helps to reduce angle random walk (ARW). This filtered output demonstrates a bias instability of 0.2 deg/hr at 1,000 sec. With future plans to both improve the resolution of the frequency detector and add active temperature control, it is expected that navigation-grade performance should be possible with the current sub-2 mm by 2 mm dies.

15. SUBJECT TERMS

Frequency control; amplitude control; resonator design and fabrication

16. SECURITY CLASSIFICATION OF:			17. LIMITATION OF ABSTRACT	18. NUMBER OF PAGES	19a. NAME OF RESPONSIBLE PERSON
a. REPORT	b. ABSTRACT	c. THIS PAGE			Andrew B. Sabater
U	U	U	SAR	36	19B. TELEPHONE NUMBER *(Include area code)* 619-553-2480

This page is intentionally blank.

This page is intentionally blank.

Naval Information Warfare Center Pacific (NIWC Pacific)
San Diego, CA 92152-5001